

# Optimal power flow solution with current injection model of generalized interline power flow controller using ameliorated ant lion optimization

Mallala Balasubbareddy<sup>1</sup>, Divyanshi Dwivedi<sup>2</sup>, Garikamukkala Venkata Krishna Murthy<sup>3</sup>,  
Kotte Sowjan Kumar<sup>3</sup>

<sup>1</sup>Department of Electrical and Electronics Engineering, Chaitanya Bharathi Institute of Technology, Hyderabad, India

<sup>2</sup>Department of Electrical and Electronics Engineering, Indian Institute of Technology, Hyderabad, India

<sup>3</sup>Department of Electrical and Electronics Engineering, PACE Institute of Technology and Sciences, Ongole, India

## Article Info

### Article history:

Received Mar 8, 2022

Revised Sep 26, 2022

Accepted Oct 8, 2022

### Keywords:

Ameliorated ant lion optimization algorithm  
Current injection modeling  
Fuel cost  
Generalized interline power flow controller  
Lehmann, Symanzik and Zimmermann formula

## ABSTRACT

Optimal power flow (OPF) solutions with generalized interline power flow controller (GIPFC) devices play an imperative role in enhancing the power system's performance. This paper used a novel ant lion optimization (ALO) algorithm which is amalgamated with Lévy flight operator, and an effectual algorithm is proposed named as, ameliorated ant lion optimization (AALO) algorithm. It is being implemented to solve single objective OPF problem with the latest flexible alternating current transmission system (FACTS) controller named as GIPFC. GIPFC can control a couple of transmission lines concurrently and it also helps to control the sending end voltage. In this paper, current injection modeling of GIPFC is being incorporated in conventional Newton-Raphson (NR) load flow to improve voltage of the buses and focuses on minimizing the considered objectives such as generation fuel cost, emissions, and total power losses by fulfilling equality, in-equality. For optimal allocation of GIPFC, a novel Lehmann-Symanzik-Zimmermann (LSZ) approach is considered. The proposed algorithm is validated on single benchmark test functions such as Sphere, Rastrigin function then the proposed algorithm with GIPFC has been testified on standard IEEE-30 bus system.

*This is an open access article under the [CC BY-SA](https://creativecommons.org/licenses/by-sa/4.0/) license.*



## Corresponding Author:

Mallala Balasubbareddy

Department of Electrical and Electronics Engineering, Chaitanya Bharathi Institute of Technology  
Hyderabad 500075, India

Email: [balasubbareddy79@gmail.com](mailto:balasubbareddy79@gmail.com)

## 1. INTRODUCTION

Optimal power flow problem aims to identify the best operating condition of a power with the fulfillment to the demand at the load side by fulfilling the considered security and practical constraints. The authors are performed particle swarm optimization (PSO) algorithm and gravitational search algorithm when tackling single-objective numerical optimization [1], [2]. Flexible alternating current transmission system (FACTS) devices plays an imperative role in optimal power flow (OPF), devices like static synchronous compensator (STATCOM), Scottish social services council (SSSC), interline power flow controller (IPFC), unified power flow controller (UPFC) and generalized interline power flow controller (GIPFC) have the better operating performance as compared to static Var compensator (SVC), thyristor controlled series capacitor (TCSC) and thyristor controlled phase shifter (TCPS) as stated in [3]–[8]. GIPFC is the latest controller which can control real and reactive power of multiple lines simultaneously, which helps to share

the load of overloaded line to unloaded line and it also helps to control the sending end voltage of transmission line at which device is placed. When we step in for implementing any FACTS device in the power system, initially power flow calculations and modification in Jacobian elements are carried out, which is possible only after mathematical modeling of considered device.

Severity function which includes line loadings and voltage violations is considered for identifying the best location for device in [9]. Sometimes installation cost of device plays a vital role thus is also considered with severity function for determining the location as considered in [10]. Here we considered a novel Lehmann, Symanzik and Zimmermann (LSZ) approach for determining the optimal location for device. Basically, it helps in calculating the voltage stability index of transmission lines in the power network [11]. Furthermore, for solving the OPF problems a handful of classical and heuristics optimization methods are being proposed by researchers in past decades. Classical methods include gradient method, linear, nonlinear, and quadratic programming, interior point and newton formulation [12]–[16].

Consider an conventional algorithm grey wolf optimization (GWO) algorithm, inspired the hunting mechanism of grey wolf as proposed in [17], is further modified to evolutionary population dynamics and grey wolf optimizer (GWO-EPD) which improves the convergence of the existing GWO algorithm with improvement in exploration and exploitation [18]. The chaotic grey wolf optimization algorithm is introduced which implement chaos theory in the GWO to improve convergence time [19]. Hybrid grey wolf optimization is proposed which is hybridization of GWO and crossover and mutation for better performance [20]. An effective grey wolf optimizer with Lévy flight (LGWO) for optimizing is proposed for improving the solution [21]. Thus, these modifications in existing GWO help to improvise the system performance. Similarly, consider another conventional algorithm artificial bee colony (ABC) optimization algorithm inspired by the intelligence behavior of honey-bee swarm in [22] and further enhanced ABC optimization [23], improved ABC algorithm for global optimization [24] and Gbest-guided ABC algorithm are proposed in [25] for enhancing the performance of conventional algorithms. Moreover, algorithms like cuckoo search algorithm (CSA) in [26] had been modified as modified cuckoo search algorithm (MCSA) in [27] and simulated annealing algorithm (SAA) in [28] had been hybridized with neighborhood generation (MSAA-NG) in [29] to ameliorate their performance and effectiveness.

Thus, a novel algorithm proposed by Mirjalili [30], named as ant lion optimization (ALO) algorithm [30], [31] is implemented with Lévy flight operator to improve its exploration. Khunkitti *et al.* [32] are proposed slime mould algorithm for solving multi-objective optimal power flow problems. Khunkitti *et al.* [33] are proposed improved dragonfly algorithm-particle swarm optimization (DA-PSO) algorithms for solving unit commitment problem. Khunkitti *et al.* [34] are described voltage stability indices in OPF. In [35] proposed hybrid DA-PSO algorithm for optimal power flow problems. It is being suggested in literature that ALO algorithm performance can further be improved by adding Lévy flight operator, as it enhances the random walk-in existing algorithm. Therefore, to enhance the performance and exploration ameliorated ant lion optimization (AALO) algorithm is being proposed. It's being validated on sphere and Rastrigin test functions to ensure that proposed algorithm possess faster convergence and solutions also get improved. The proposed algorithm is validated on the standard-test function and then optimal power flow problem is being solved with proposed method. Thus, this paper presents derivation of current injection modeling (CIM) of GIPFC which is incorporated in conventional Newton-Raphson (NR) load flow method with its optimal allocation through LSZ approach and aims to solve the single-objective OPF problem under practical constraints for standard IEEE-30 bus system using proposed AALO algorithm respectively.

## 2. MATHEMATICAL MODELING OF GIPFC

GIPFC is a static convertible controller which has the ability to control the multiple lines simultaneously. The basic arrangement of GIPFC is depicted in Figure 1. Assume that the device is located between buses  $i$ ,  $j$ ,  $m$ , and  $n$ . Basically it consists of two series converters which are placed at two different transmission lines which are coupled through a shunt converter placed at the sending end side of any one of the contemplated transmission lines.

### 2.1. Current injection modeling of GIPFC

The current based model of GIPFC is shown in Figure 2, and the two flowing currents can be written as (1):

$$\bar{I}_{se,ij} = jB_{se,ij}(\bar{V}_{se,ij}), \bar{I}_{se,mn} = jB_{se,mn}(\bar{V}_{se,mn}), \bar{I}_{sh} = jB_{sh}(\bar{V}_{sh}) \quad (1)$$

where,  $\bar{V}_{se,ij} = V_{se,ij}e^{j\theta_{se,ij}}$ ,  $\bar{V}_{se,mn} = V_{se,mn}e^{j\theta_{se,mn}}$  and  $\bar{V}_{sh} = V_{sh}e^{j\theta_{sh}}$ ;  $\bar{I}_{se,ij}$  and  $\bar{I}_{se,mn}$  are the series converter currents operating in ranges of  $0 \leq V_{se} \leq V_{se,max}$  and  $0 \leq \theta_{se} \leq \theta_{se,max}$ .  $\bar{I}_{sh}$  is the shunt converter

current operating in range of  $0 \leq V_{sh} \leq V_{sh,max}$  and  $0 \leq \theta_{sh} \leq \theta_{sh,max}$ .  $B_{se,ij}$ ,  $B_{se,mn}$  are the susceptance of series converters and  $B_{sh}$  is the susceptance of shunt converter.

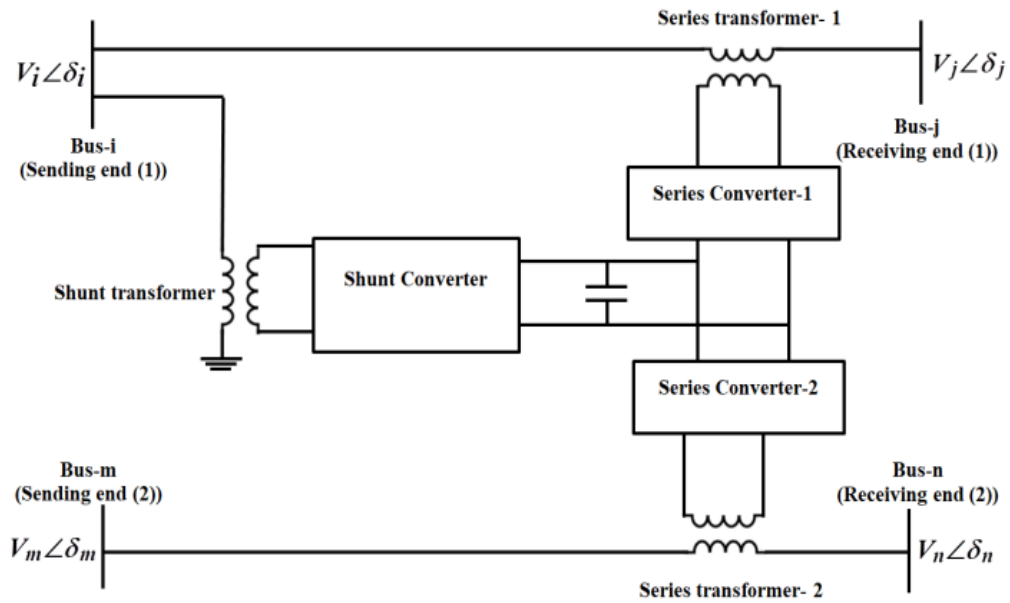


Figure 1. Basic arrangement of GIPFC

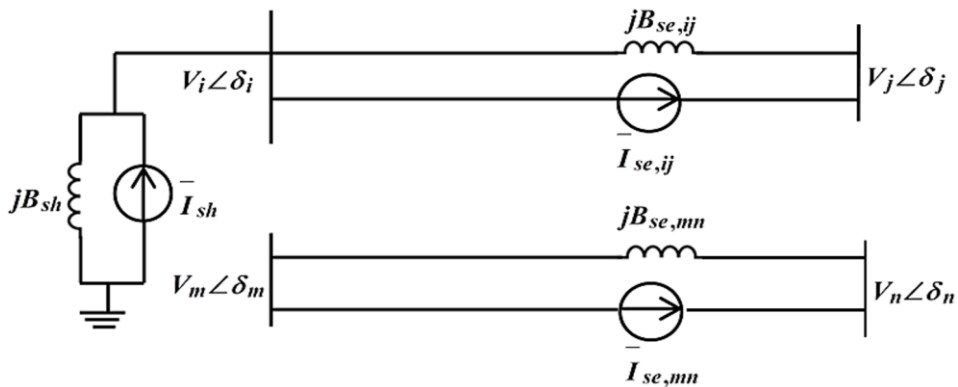


Figure 2. Current based model of GIPFC

Current injected in transmission line between  $i^{th}$  and  $j^{th}$  buses can be expressed as (2):

$$\bar{I}_{ij} = (\bar{V}_i - \bar{V}_j + \bar{V}_{se,ij})jB_{se,ij} + \bar{V}_sh jB_{sh} \tag{2}$$

Current injected in transmission line between  $m^{th}$  and  $n^{th}$

$$\bar{I}_{mn} = (\bar{V}_m - \bar{V}_n + \bar{V}_{se,mn})jB_{se,mn} \tag{3}$$

where,  $\bar{V}_i = V_i e^{j\delta_i}$ ,  $\bar{V}_j = V_j e^{j\delta_j}$ ,  $\bar{V}_m = V_m e^{j\delta_m}$  and  $\bar{V}_n = V_n e^{j\delta_n}$  are the bus voltages.

a) GIPFC injecting power at Bus-i

$$\bar{S}_{si} = P_{si} + jQ_{si} = \bar{V}_i (\bar{I}_{ij})^*$$

Substituting from (2) and on solving we get

$$P_{si} = V_i V_j B_{se,ij} \sin \delta_{ij} - V_i V_{se,ij} B_{se,ij} \sin(\delta_i - \theta_{se,ij}) - V_i V_{sh} B_{sh} \sin(\delta_i - \theta_{sh}) \quad (4)$$

where,  $\delta_{ij} = \delta_i - \delta_j$

$$Q_{si} = V_i V_j B_{se,ij} \cos \delta_{ij} - V_i V_{se,ij} B_{se,ij} \cos(\delta_i - \theta_{se,ij}) - V_i V_{sh} B_{sh} \cos(\delta_i - \theta_{sh}) - V_i^2 B_{se,ij} \quad (5)$$

b) GIPFC injecting power at Bus-j

$$\bar{S}_{sj} = P_{sj} + jQ_{sj} = \bar{V}_j (-\bar{I}_{ij})^*$$

On solving we get

$$P_{sj} = -V_i V_j B_{se,ij} \sin \delta_{ij} + V_j V_{se,ij} B_{se,ij} \sin(\delta_j - \theta_{se,ij}) \quad (6)$$

$$Q_{sj} = V_i V_j B_{se,ij} \cos \delta_{ij} + V_j V_{se,ij} B_{se,ij} \cos(\delta_j - \theta_{se,ij}) - V_j^2 B_{se,ij} \quad (7)$$

c) GIPFC injecting power at Bus-m

$$\bar{S}_{sm} = P_{sm} + jQ_{sm} = \bar{V}_m (\bar{I}_{mn})^*$$

Substituting from (3) and on solving we get

$$P_{sm} = V_m V_n B_{se,mn} \sin \delta_{mn} - V_m V_{se,mn} B_{se,mn} \sin(\delta_m - \theta_{se,mn}) \quad (8)$$

where,  $\delta_{mn} = \delta_m - \delta_n$

$$Q_{sm} = V_m V_n B_{se,mn} \cos \delta_{mn} - V_m V_{se,mn} B_{se,mn} \cos(\delta_m - \theta_{se,mn}) - V_m^2 B_{se,mn} \quad (9)$$

d) GIPFC injecting power at Bus-n

$$\bar{S}_{sn} = P_{sn} + jQ_{sn} = \bar{V}_n (-\bar{I}_{mn})^*$$

On solving we get

$$P_{sn} = -V_m V_n B_{se,mn} \sin \delta_{mn} + V_n V_{se,mn} B_{se,mn} \sin(\delta_n - \theta_{se,inn}) \quad (10)$$

$$Q_{sn} = V_m V_n B_{se,mn} \cos \delta_{mn} + V_n V_{se,mn} B_{se,mn} \cos(\delta_n - \theta_{se,mn}) - V_n^2 B_{se,mn} \quad (11)$$

## 2.2. Power mismatches equations of GIPFC

The proposed current injection model of GIPFC is easily incorporated into the system by modifying the Jacobian elements and power mismatch equations related to device connected buses. The existing Jacobian elements obtained from NR is modified by adding the variational derivative of real and reactive power occurring because of the incorporation of GIPFC. The final equation of NR load flow with GIPFC can be expressed as (12):

$$\begin{pmatrix} \Delta P \\ \Delta Q \end{pmatrix} + \begin{pmatrix} P^{GIPFC} \\ Q^{GIPFC} \end{pmatrix} = \begin{pmatrix} H & N \\ J & L \end{pmatrix} + \begin{pmatrix} H^{GIPFC} & N^{GIPFC} \\ J^{GIPFC} & L^{GIPFC} \end{pmatrix} \begin{pmatrix} \Delta \delta \\ \frac{\Delta V}{|V|} \end{pmatrix} \quad (12)$$

where,

$\Delta P, \Delta Q$ : the vectors representing real and reactive power mismatches,  
 $\Delta \delta, \Delta V$ : the vectors of incremental change in the angles and voltages,  
 $H, N, J, L$ : the partial derivative of P and Q with respect to  $\delta$  and V.

### 2.3. Jacobian elements related to CIM of GIPFC

Elements of H:

$$\frac{\partial P_{si}}{\partial \delta_i} = V_i V_j B_{se,ij} \cos \delta_{ij} - V_i V_{se,ij} B_{se,ij} \cos(\delta_i - \theta_{se,ij}) - V_i V_{sh} B_{sh} \cos(\delta_i - \theta_{sh})$$

$$\frac{\partial P_{si}}{\partial \delta_j} = -V_i V_j B_{se,ij} \cos \delta_{ij}, \quad \frac{\partial P_{si}}{\partial \delta_m} = \frac{\partial P_{si}}{\partial \delta_n} = \frac{\partial P_{sj}}{\partial \delta_m} = \frac{\partial P_{sj}}{\partial \delta_n} = 0, \quad \frac{\partial P_{sj}}{\partial \delta_i} = -V_i V_j B_{se,ij} \cos \delta_{ij}$$

$$\frac{\partial P_{sj}}{\partial \delta_j} = V_i V_j B_{se,ij} \cos \delta_{ij} + V_j V_{se,ij} B_{se,ij} \cos(\delta_j - \theta_{se,ij})$$

$$\frac{\partial P_{sm}}{\partial \delta_m} = V_m V_n B_{se,mn} \cos \delta_{mn} - V_m V_{se,mn} B_{se,mn} \cos(\delta_m - \theta_{se,mn})$$

$$\frac{\partial P_{sm}}{\partial \delta_n} = -V_m V_n B_{se,mn} \cos \delta_{mn}, \quad \frac{\partial P_{sm}}{\partial \delta_i} = \frac{\partial P_{sm}}{\partial \delta_j} = \frac{\partial P_{sn}}{\partial \delta_i} = \frac{\partial P_{sn}}{\partial \delta_j} = 0, \quad \frac{\partial P_{sn}}{\partial \delta_m} = -V_m V_n B_{se,mn} \cos \delta_{mn}$$

$$\frac{\partial P_{sn}}{\partial \delta_n} = V_m V_n B_{se,mn} \cos \delta_{mn} + V_n V_{se,mn} B_{se,mn} \cos(\delta_n - \theta_{se,mn})$$

Elements of N:

$$\frac{\partial P_{si}}{\partial V_i} |V_i| = V_j B_{se,ij} \sin \delta_{ij} - V_{se,ij} B_{se,ij} \sin(\delta_i - \theta_{se,ij}) - V_{sh} B_{sh} \sin(\delta_i - \theta_{sh})$$

$$\frac{\partial P_{si}}{\partial V_j} |V_j| = V_i B_{se,ij} \sin \delta_{ij}, \quad \frac{\partial P_{si}}{\partial V_m} |V_m| = \frac{\partial P_{si}}{\partial V_n} |V_n| = \frac{\partial P_{sj}}{\partial V_m} |V_m| = \frac{\partial P_{sj}}{\partial V_n} |V_n| = 0,$$

$$\frac{\partial P_{sj}}{\partial V_i} |V_i| = -V_j B_{se,ij} \cos \delta_{ij}$$

$$\frac{\partial P_{sj}}{\partial V_j} |V_j| = -V_i B_{se,ij} \sin \delta_{ij} + V_{se,ij} B_{se,ij} \sin(\delta_j - \theta_{se,ij})$$

$$\frac{\partial P_{sm}}{\partial V_m} |V_m| = V_n B_{se,mn} \sin \delta_{mn} - V_{se,mn} B_{se,mn} \sin(\delta_m - \theta_{se,mn})$$

$$\frac{\partial P_{sm}}{\partial V_n} |V_n| = V_m B_{se,mn} \sin \delta_{mn}, \quad \frac{\partial P_{sm}}{\partial V_i} |V_i| = \frac{\partial P_{sm}}{\partial V_j} |V_j| = \frac{\partial P_{sn}}{\partial V_i} |V_i| = \frac{\partial P_{sn}}{\partial V_j} |V_j| = 0, \quad \frac{\partial P_{sn}}{\partial V_m} |V_m| = -V_n B_{se,mn} \sin \delta_{mn}$$

$$\frac{\partial P_{sn}}{\partial V_n} |V_n| = -V_m B_{se,mn} \sin \delta_{mn} + V_{se,mn} B_{se,mn} \sin(\delta_n - \theta_{se,imn})$$

Similarly, we can obtain the Jacobian elements for reactive power by partially differentiating (8)-(11) with respect to  $\delta$  and  $V$ .

### 3. OPTIMAL ALLOCATION OF GIPFC

This paper is inspired by a novel approach for identifying the best suitable location for GIPFC named as, LSZ formula. It helps in determining the voltage stability limit of the load buses present in power system and identify the buses which can suffer from voltage collapse. Usually, critical buses are identified in terms of maximum load ability. Consider a single line diagram of two bus system shown in Figure 3.

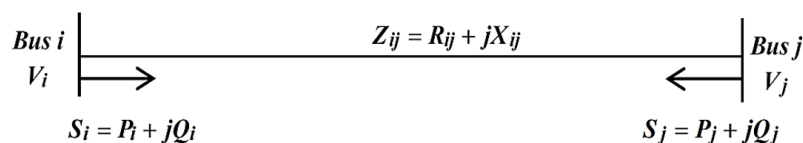


Figure 3. Single line diagram of two bus system

Where,  $v_i$ ,  $v_j$  are the sending and receiving end voltages respectively,  $Z_{ij}$  is the impedance of transmission line,  $S_i$ ,  $S_j$  is the sending and receiving end apparent powers respectively. Thus, LSZ formula obtained from [11] is:

$$LSZFormula = 2 \times \frac{|Z_{ij}| |S_j|}{|V_i|^2 - 2|Z_{ij}|(P_j \cos \theta + Q_j \sin \theta)} \leq 1$$

In this, weakest transmission line of power system is being identified which could be in critical state and more likely to collapse and has the largest value for the LSZ formula. This identified transmission required external support thus it would be considered as the optimal line to place the GIPFC device. In this paper, some heuristic rules are considered for reducing the number of possible locations for GIPFC: i) device should not be placed at PV buses; ii) there should not be any shunt compensating device present; and iii) lines in which tap changing transformers are already present should be avoided

#### 4. PROBLEM FORMULATION OF OPF

Basically, OPF problem is implemented for optimizing the objective function under the consideration of some below mentioned constraints. OPF can be expressed as:

$$\text{Min } J_p(a, b) \quad \forall p = 1, 2, \dots, O_f$$

$$\text{Subject to: } u(a, b) = 0$$

$$vmax_{min}$$

where,  $u$  and  $v$  represent equality and inequality constraints respectively,  $a$  represents state vector of dependent variables and  $b$  represents control vector of system and  $O_f$  represents total number of objective functions. The state vector can be represented by:

$$a^T = [P_{g_1}, V_{l_1}, \dots, V_{l_{NPQ}}, Q_{g_1}, \dots, Q_{g_{NPV}}, S_{l_1}, \dots, S_{l_{NTL}}]$$

The control vector can be represented by:

$$b^T = [P_{g_2}, \dots, P_{g_{NPV}}, V_{g_1}, \dots, V_{g_{NPV}}, Q_{sh_1}, \dots, Q_{sh_{NC}}, T_{t_1}, \dots, T_{t_{NT}}]$$

where,  $P_{g_1}$ ,  $V_{l_1}$ ,  $Q_{g_1}$ ,  $S_{l_1}$  and  $V_{g_1}$  are the active power, load bus voltage, reactive power, apparent power, and generator voltage of slack bus respectively. NPQ, NPV, NTL, NC and NT are the total number of PQ buses, PV buses, transmission lines, shunt compensators and off-nominal taps transformers respectively.

##### 4.1. Objective functions

In this paper, three single objective functions are considered for minimization, which is mathematically expressed:

- Generation fuel cost minimization

$$J_1 = \min(F_c(P_{g_m})) = \sum_{m=1}^{NPV} x_m P_{g_m}^2 + y_m P_{g_m} + z_m \$/h \quad (13)$$

where,  $x_m$ ,  $y_m$  and  $z_m$  are the fuel cost coefficients of  $m^{th}$  unit.

- Emission minimization

$$J_2 = \min(E(P_{g_m})) = \sum_{m=1}^{NPV} \alpha_m + \beta_m P_{g_m} + \gamma_m P_{g_m}^2 + \xi_m \exp(\lambda_m P_{g_m}) \text{ ton/h} \quad (14)$$

where,  $\alpha_m$ ,  $\beta_m$ ,  $\gamma_m$ ,  $\lambda_m$  and  $\xi_m$  are the emission coefficients of  $m^{th}$  unit.

- Total power loss minimization

$$J_3 = \min(P_{loss}) = \sum_{m=1}^{NTL} P_{loss_m} \text{ MW} \quad (15)$$

where,  $P_{loss_m}$  is the real power loss in  $m^{th}$  line.

## 4.2. Constraints

Basically, OPF with FACTS device is subjected to equality, in-equality, and device constraints. The in-equality constraints include generator, transformer, shunt compensator operating constraints depending upon various system parameters. In this paper, practical constraints are also considered such as ramp-rate limits and prohibited operating zone (POZ).

### 4.2.1. Equality constraints

The optimization of objective functions must satisfy the equality constraint as given bellow.

$$\sum_{m=1}^{NPV} P_{g_m} - P_d - P_l = 0, \quad \sum_{m=1}^{NPV} Q_{g_m} - Q_d - Q_l = 0$$

where,  $P_d$ ,  $Q_d$  and  $P_l$ ,  $Q_l$  are the real and reactive demands and losses respectively.

### 4.2.2. Inequality constraints

The said objective function optimization the following in-equality constraints must satisfy. The in-equality constraints as given bellow.

a) Generator constraints. All the buses with generators including slack bus are bounded by the voltages, real and reactive powers limits as expressed:

$$V_{g_m}^{\min_{g_m} \max}, P_{g_m}^{\min_{g_m} \max} \text{ and } Q_{g_m}^{\min_{g_m} \max} \quad \forall m \in NPV$$

b) Tap changing transformers constraints

$$T_{t_m}^{\min_{t_m} \max} \quad \forall m \in NT$$

c) Shunt compensators constraints

$$S_{sh_m}^{\min_{sh_m} \max} \quad \forall m \in NC$$

d) Security constraints. Voltages at all the PQ buses must be restricted within a specified range and line flows in transmission line should not violate the maximum limit.

$$V_{l_m}^{\min_{l_m} \max} \quad \forall m \in NPQ$$

$$S_{l_m} \leq S_{l_m}^{\max} \quad \forall m \in NTL$$

e) GIPFC constraints. GIPFC is restricted in terms of injected series and shunt voltages magnitudes, phase angles and reactance.

$$0 \leq V_{se} \leq 0.1, 0 \leq \theta_{se} \leq 360^\circ, 0 \leq X_{se} \leq 0.1, 0 \leq V_{sh} \leq 0.1, 0 \leq \theta_{sh} \leq 360^\circ, 0 \leq X_{sh} \leq 0.1$$

f) Ramp-rate limits. The ramp-rate limits of  $m^{th}$  generator in MW/hour are as shown:

$$\max(P_{g_m}^{\min_{g_m}^0}, \min_{g_m}^{\max_{g_m}^0})$$

where,  $P_{g_m}^0$  is the generated power in previous hour,  $R_1$  and  $R_2$  are the up-rate and down-rate limit of  $m^{th}$  generator.

g) POZ limits. In power systems, POZ limits generator operation in certain ranges from the entire range of possible generation. For  $m^{th}$  generator POZ at each time interval can be formulated as:

$$P_{g_m}^{\min_{g_m}^L}$$

$$P_{g_{m(p-1)}}^U \leq P_{g_m} \leq P_{g_{m(p)}}^L$$

$$P_{g_{m(n)}}^U \leq P_{g_m} \leq P_{g_m}^{max}$$

where,  $n$  is the number of prohibited zones,  $p$  is the index for prohibited zones,  $P_{g_{m(p)}}^L$  and  $P_{g_{m(p)}}^U$  are the lower and upper limit of  $p^{th}$  prohibited zone for  $m^{th}$  generator. With these constraints a penalty function is also incorporated to the objective function; it will allocate the initial values of penalty weights if constraints violate their limits [32].

## 5. AMELIORATED ANT LION OPTIMIZATION ALGORITHM

### 5.1. Existing ant lion optimization algorithm

ALO algorithm is an optimization algorithm inspired by natural phenomenon and proposed in [31]. It mimics the hunting mechanism of ant lions. It is a novel meta-heuristic algorithm that is dwelt mathematically through the interaction between ants (prey) and ant lions (predator). Ant lions are the doodlebugs which basically belong to the *Myrmeleontidae* family, they possess two phases of life in 3 years of their total life span i.e., larvae for just 3-5 weeks and remaining is adult phase. In the phase of larvae their hunting mechanism is very fascinating. Initially, they start building cone shaped traps by throwing sand out with its jaw, and then they wait for ants at the edge of the conical structure to be get trapped into it, as shown in Figure 4. The stimulating features of these ant lions for digging traps are the hunger level and shapes of the moon. They used to dig a bigger trap in hunger and in full-shaped moon, which enhances the probability of their survival. ALO yields for global optimum solutions for constraint bounded optimization problems. It also maintains equilibrium among exploration and exploitation, with faster convergence [36].

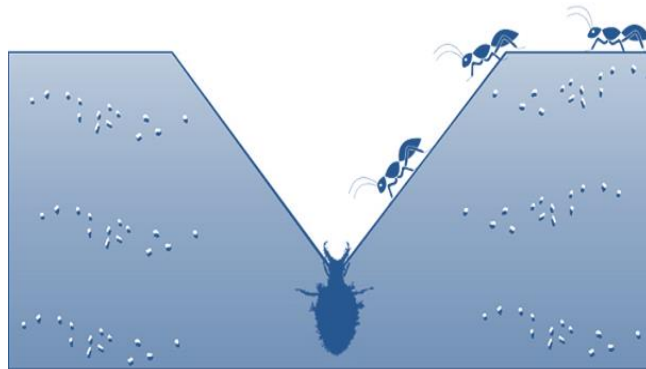


Figure 4. Cone shaped trap for hunting ants

### 5.2. Proposed ameliorated ant lion optimization algorithm

Basically ALO is implemented in five stages, which includes the complete mechanism of antlions' hunting and further in the existing algorithm the Lévy flight operator of Cuckoo Search algorithm [27] has been added to ameliorate the overall performance. Main steps of proposed algorithm are being described with mathematical equations below.

#### 5.2.1. Stochastic walk of ants

Initially, ants move erratically in search of food, which can be modeled:

$$A(r) = [0, cs(2w(r_1) - 1), cs(2w(r_2) - 1), \dots, cs(2w(r_{IT}) - 1)] \quad (16)$$

where,  $cs$  stands for cumulative sum,  $r$  is the step of random walks,  $IT$  maximum number of iterations and  $w(t)$  can be considered as (17):

$$w(r) = \begin{cases} 1, & \text{if rand} > 0.5 \\ 0, & \text{if rand} \leq 0.5 \end{cases} \quad (17)$$

The positions of ants are saved in matrix as:

$$X_{Ant} = \begin{bmatrix} Ant_{11} & Ant_{12} & \dots & Ant_{1D} \\ Ant_{21} & Ant_{22} & \dots & Ant_{2D} \\ \vdots & \vdots & \vdots & \vdots \\ Ant_{N1} & Ant_{N1} & \dots & Ant_{ND} \end{bmatrix}$$

where,  $X_{Ant}$  matrix which have position of each ant,  $Ant_{xy}$  represents the value of  $x^{th}$  ants for  $y^{th}$  dimension,  $N$  and  $D$  are total number of ants (search variables) and dimension respectively. Therefore, the random walks can be normalized so that they are inside the search space.

$$A_i^t = \frac{(A_i^t - m_i) \times (k_i^t - j_i^t)}{n_i - m_i} + j_i^t \quad (18)$$

where,  $m_i$  and  $n_i$  are the minimum and maximum of walk of  $i^{th}$  variable,  $j_i^t$  and  $k_i^t$  are the minimum and maximum of walk of  $i^{th}$  variable at  $t^{th}$  iteration.

### 5.2.2. Ants trapped in ant lions' traps

Ant lion's pits have their impact on the erratic walks of ants. To mathematically model this assumption the following equations are used:

$$j_i^t = AntLion_j^t + j^t \quad (19)$$

$$k_i^t = AntLion_j^t + k^t \quad (20)$$

where,  $j_i^t$  and  $k_i^t$  minimum and maximum of all variables at  $t^{th}$  iteration respectively.  $AntLion_j^t$  is the position of selected  $j^{th}$  ant lion at  $t^{th}$  iteration.

### 5.2.3. Building the traps

Roulette wheel selection is used for building the traps. Basically, in optimization the roulette wheel operator helps in selecting the ant lions based on their fitness. The chance of ants getting caught by the fitter ant lions is more.

### 5.2.4. Slipping ants in the direction of ant lion

Ant lions always build the trap accordance to their fitness and the ants usually reach the search space randomly. When the ants enter into the pit the ant lions throw the sand outwards so that ants can slip towards ant lions. The radius of ant's erratic walk is represented as (21), (22):

$$j^t = \frac{j^t}{Z} \quad (21)$$

$$k^t = \frac{k^t}{Z} \quad (22)$$

where,  $Z = \frac{10^{Kt}}{IT}$ , in which  $t$  and  $IT$  are current and maximum number of iterations respectively.  $K$  is a constant weight defined based on the basis of current iteration ( $K=2$  when  $t > 0.1IT$ ,  $K=3$  when  $t > 0.5IT$ ,  $K=4$  when  $t > 0.75IT$ ,  $K=5$  when  $t > 0.9IT$ ,  $K=6$  when  $t > 0.95IT$ ).

### 5.2.5. Hunting ant then revamp the pit

The terminating stage will occur when ant being caught by the ant lions, and it is made possible only when the ant becomes fitter than the corresponding ant lion. Then antlion should amend their position towards current position where ant gets hunted so that it enhances the probability of catching another ant. This phenomenon can be expressed as (23):

$$AntLion_j^t = Ant_i^t \text{ if } f(Ant_i^t) > f(AntLion_j^t) \quad (23)$$

where,  $Ant_j^t$  is the position of selected  $i^{th}$  ant at  $t^{th}$  iteration.

**5.2.6. Elitism**

Elitism is a salient operation of the evolutionary algorithms. It basically facilitates to obtain the optimal solution for the considered problems. For each iteration, best ant lion will be identified and contemplated as Elite, which will affect the movements of ants. It can be mathematically modeled as (24):

$$Ant_i^t = \frac{(Q_A^t + Q_E^t)}{2} \tag{24}$$

where,  $Q_A^t$  and  $Q_E^t$  random walk around the ant lion and elite selected at  $t^{th}$  iteration.

**5.2.7. Lévy flight operator**

Random walk of ants is being updated using Lévy flight operator from CSA, which enhances performance of existing algorithm. As the Lévy flight operator makes exploration more effective, it can be calculated as (25):

$$Lévy(\alpha) = \left| \frac{\Gamma(1+\alpha) \times \sin(0.5\pi\alpha)}{\Gamma(\frac{1+\alpha}{2}) \times \alpha \times 2^{0.5(\alpha-1)}} \right|^{\frac{1}{\alpha}} \tag{25}$$

where,  $\alpha$  is a constant whose value considered to be equal to 1.5 [37] and  $\Gamma$  is a gamma distribution function. Thus, it updates the random walk of ants by (26):

$$A_i^t = m_i + Lévy \times (n_i - m_i) \tag{26}$$

**6. RESULTS AND ANALYSIS**

**6.1. Benchmark test functions**

In this section, two benchmark test functions are preferred to validate the proposed algorithm. First function F (1) is a Sphere function, and second function F (2) is a Rastrigin function, both the functions are continuous, differential, separable and can be defined for N-dimension space, only difference is that sphere function is a unimodal function while Rastrigin function is a multimodal function. Parameters setting for both the test functions are listed in Table 1.

Table 1. Parameters setting for Sphere and Rastrigin functions

Function	Dimension	Range	No. of search variables	Max. Iteration
$F(1) = \sum_{i=1}^n x_i^2$	30	[-100,100]	40	100
$F(2) = \sum_{i=1}^n x_i^2 - 10 \cos(2\pi x_i) + 10$	30	[-5.12, 5.12]	40	100

From Table 2, it can be seen that the results achieved for both the test functions when proposed AALO algorithm is implemented are less than the existing algorithms. For the sphere function, output is 4.0681e-11 which is approximately 2.1832e-10 less than the output obtained through ALO algorithm. Similarly, for the Rastrigin function output is 7.437e-07 which is less than the output obtained through ALO algorithm. In Table 2 some of the existing algorithms like bat algorithm (BA), s-metric selection (SMS), hybrid cuckoo search algorithm (HCSA) are compared with proposed method.

Table 2. Comparison of optimal result obtained for the Sphere and Rastrigin functions

Function	Existing BA [31]	Existing SMS [31]	Existing PSO [31]	HCSA	Existing ALO [31]	Proposed AALO
Sphere Function	0.77362	0.0569	2.70e-09	6.83e-10	2.59e-10	4.0681e-11
Rastrigin Function	1.23374	1.3251	0.278588	4.012 e -03	7.71e-06	7.437e-07

From Figures 5-6 it can be analyzed that, initial iteration starts with lesser value in case of the AALO algorithm in comparison to the existing algorithms for both the benchmark test functions. It can also

be observed that convergence curve of proposed algorithm shows a smooth variation while for ALO algorithm curve has stepped variations. The optimum value obtained for both the functions are achieved in less iteration as compared to existing algorithms. Thus, it can be concluded that with the proposed AALO algorithm converges very fast for multi-modal as well as unimodal test function and it efficiently solve the multi-modal test function problems with the avoidance of local optima, so for further analysis AALO algorithm is preferred.

**6.2. Electrical test system**

In order to justify the robustness and effectiveness of the proposed algorithm, IEEE-30 bus system is considered for solving the single objective OPF problem, in which 6 generators are placed at 1, 2, 5, 8, 11 and 13 and remaining are the PQ buses. It consists of 41 transmission lines, 18 control variables, 4 transformers are placed between buses 6-9, 6-10, 4-12, 28-27 and two shunt devices are located at buses 10 and 24. Required bus data, line data, load data, cost data and generation data has been considered from [38].

Optimal power flow results for generation fuel cost with implementation of proposed AALO algorithm is tabulated in Table 3, with its comparison from the existing algorithms. It can be seen that generation fuel cost is minimized to 789.462\$/h which is by far the better solution obtained in comparison to other existing algorithms. The proposed algorithm compared with existing method such as fruit fly algorithm (FFA), hybrid cuckoo search algorithm (HCSA), modified sine-cosine algorithm (MSCA).

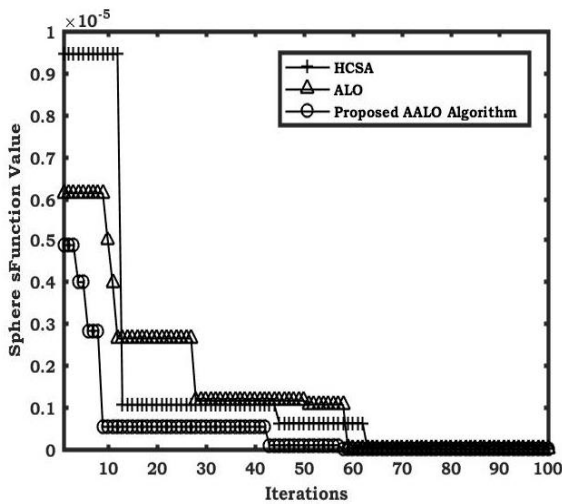


Figure 5. Convergence curve for the Sphere test function with different algorithms

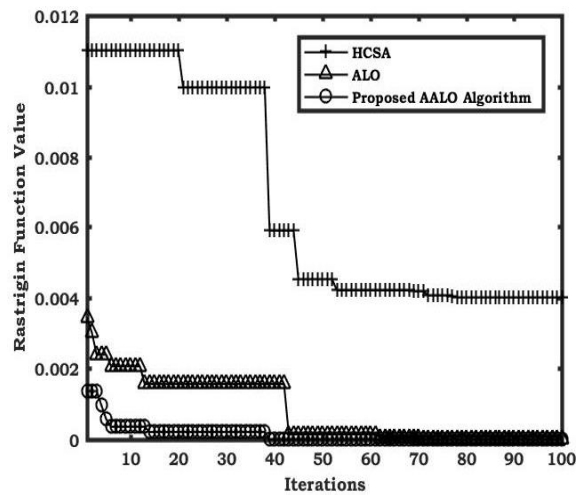


Figure 6. Convergence curve for the Rastrigin test function with different algorithms

Table 3. Comparison of OPF solutions for generation fuel cost minimization for IEEE-30 bus system

Variables	PSO [9]	FFA [39]	ALO	HCSA [40]	EMA [41]	MSCA [42]	Proposed AALO
PG1, MW	178.5558	177.7152	176.6491	176.87	177.258	177.401	175.969
PG2, MW	48.6032	45.46423	48.83991	49.8862	48.4	48.632	48.12035
PG5, MW	21.6697	22.24322	21.52671	21.6135	21	21.2376	25.18808
PG8, MW	20.7414	20.59715	21.73635	20.8796	21.606	20.8615	15.97765
PG11, MW	11.7702	14.70965	12.16658	11.6168	12.012	11.9385	18.6224
PG13, MW	12	12	12	12	12	12	14.30414
V1, p.u.	1.1	1.098934	1.1	1.057	1.1	1.1	1.055672
V2, p.u.	0.9	1.082836	1.07135	1.0456	1.1	1.0867	0.981154
V5, p.u.	0.9642	0.919706	1.06827	1.0184	1.0487	1.0604	0.954773
V8, p.u.	0.9887	1.1	1.0735	1.0265	1.0504	1.0923	0.966615
V11, p.u.	0.9403	0.961242	0.95708	1.057	1.0725	1.1	0.975921
V13, p.u.	0.9284	1.062683	1.03229	1.057	1.0461	1.1	0.9
T 6-9, p.u.	0.9848	1.006858	1	1.0254	0.9858	1.0439	0.983995
T 6-10, p.u.	1.0299	0.993187	1.08182	0.9726	1.0229	0.9144	0.993805
T 4-12, p.u.	0.9794	0.990804	1.1	1.006	1.0085	1.03	0.944875
T 28-27, p.u.	1.0406	0.981178	1.03477	0.9644	0.9973	0.9913	0.946326
Q 10, p.u.	9.0931	28.98477	15.0667	25.3591	0.02893	0.0246	6.505655
Q 24, p.u.	21.665	20.53278	9.5678	10.6424	0.01084	4.8426	10.15237
Fuel cost \$/h	803.454	802.3834	802.2029	802.034	799.963	799.31	798.4617

In Figure 7 convergence curve of generation fuel cost is shown which clearly shows that the proposed algorithm converges fast as compared to existing methods. For validating the effectiveness of proposed algorithm, results available from literature is shown in Table 4, from the best minimum result is obtained using proposed AALO algorithm. So, for further analysis AALO algorithm will be considered.

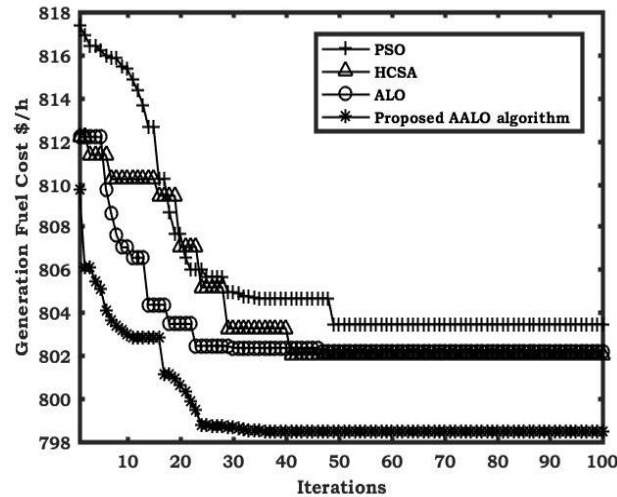


Figure 7. Convergence curve of generation fuel cost with different algorithms

Table 4. Summarized result for generation fuel cost minimization for IEEE-30 bus system

Existing Methods	Fuel cost in \$/h
Bees two-hive [43]	798.466
Enhanced genetic algorithm (EGA) [42]	802.06
Modified shuffle frog leaping algorithm (MSFLA) [44]	802.287
Chaotic self-adaptive differential HSA (CDHSA) [45]	801.588
Monarch butterfly optimization (MBO) [46]	823.3999
Gbest-guided cuckoo search algorithm [47]	800.4173
Gradient method [48]	804.853
HCSA [9]	802.0347
TS [49]	802.29
Backtracking search algorithm [50]	801.63
DA-PSO [35]	802.1241
Ant colony optimization (ACO) [51]	802.5780
Gravitational search algorithm (GSA) [52]	798.6751
Biogeography-based optimization (BBO) [53]	799.1116
Differential evolution algorithm [48]	799.289
Novel Improved Social Spider Optimization (NISSO) [1]	799.76242

### 6.3. Incorporation of GIPFC device in IEEE-30 bus system

Now we will incorporate the GIPFC devices in our electric test system but before that we need to identify the weakest buses in IEEE-30 bus system so that GIPFC can be optimally placed at those buses to enhance the system parameters. For determination of weakest line, LSZ method is applied, and whichever lines get maximum LSZ value will be considered to be the weakest bus and rank high in order. For all the lines LSZ is calculated which are mentioned in Table 5, from which we can see that line 7 between the buses 5-7 is the weakest bus in test system but as per considered heuristic rule, it cannot be considered to place GIPFC as bus 5 is a PV bus, so next weakest line is 39 which is between buses 29-30. Next lines 5 and 3 which are between buses 2-5 and 2-4 respectively also cannot be considered as bus 2 is also a PV bus. Then second line which can be selected is 32 which are between buses 24-25. So, lines between the buses 24-25 and 29-30 are taken as the weakest line and optimal location to place GIPFC.

After determining the weakest buses, GIPFC is incorporated in NR load flow to overcome the shortcomings caused due to the weak lines. The OPF solution for considered objectives are mentioned in Table 6, in this table three cases are compared, one without placing any FACTS device, second are with incorporation of IPFC and third is with incorporation of GIPFC. It can be seen from the Table 6, that objectives get reduced to lesser value when IPFC [9] and GIPFC are incorporated in comparison to the system without any FACTS controller. We can also observe and conclude that among both the devices i.e.,

IPFC and GIPFC, OPF solution for considered objectives are least when GIPFC is incorporated. Generation fuel cost got minimized to 800.3032\$/h, emission got minimized to 0.20496 ton/h and total power loss got minimized to 3.271884 MW when GIPFC is incorporated (all results obtained is under both the practical constraints). From this result GIPFC controller is superior and more efficient as compared to IPFC controller. So GIPFC is being carried forward for further analysis.

Table 5. Rank orders of weakest lines with its LSZ value

Line No.	Between Buses	LSZ Output	Rank
7	5-7	16.73588	1
39	29-30	11.597432	2
5	2-5	9.4938832	3
3	2-4	9.3499862	4
32	24-25	8.3311588	5
16	12-13	7.6553758	6
18	12-15	5.9315986	7
21	16-17	4.1713139	8
17	12-14	3.9424517	9
29	21-22	3.8644979	10
19	12-16	3.8144801	11
15	4-12	3.7741881	12
14	9-10	3.5390679	13
24	19-20	2.809922	14
38	27-30	2.6291642	15
31	22-24	2.1504857	16
27	10-21	2.0442206	17
20	14-15	1.646794	18
23	18-19	1.5342253	19
25	10-20	1.1104449	20
28	10-22	1.0927438	21
26	10-17	1.0133989	22
22	15-18	0.9582758	23
6	2-6	0.595508	24

Table 6. Comparison of OPF solutions with and without FACTS devices for IEEE-30 bus system

Variables	Generation fuel cost \$/h			Emission ton/h			Total power loss (MW)		
	Without FACTS	With IPFC [9]	With GIPFC	Without FACTS	With IPFC [9]	With GIPFC	Without FACTS	With IPFC [9]	With GIPFC
PG1, MW	173.267	158.75	152.145	74.54	63.41	51.2181	66.9994	65.42	71.283
PG2, MW	50	46.41	60	60.5741	68.9981	50	67.9175	71.0932	25
PG5, MW	36.6578	20.13	22.7398	27.6277	50	29.4145	47.9556	50	39.5605
PG8, MW	20.5048	25	21.4135	17.098	35	21.2359	35	35	24.0324
PG11, MW	28.4988	24.1985	16.1379	18.2864	30	28	25	30	16.7638
PG13, MW	23.1682	15.213	18.8414	38.441	40	35	35.4886	35.3123	24
V1, p.u.	0.94967	1.0039	0.99398	1.0476	0.9914	0.9824	1.0625	1.1	1.09219
V2, p.u.	0.9027	0.9556	0.9679	1.01244	0.95	0.96137	0.98534	1.1	0.99392
V5, p.u.	0.93732	1.0118	1.08174	0.95137	0.9854	0.99058	1.03854	1.0677	1.04351
V8, p.u.	0.93537	0.9923	1.0096	1.00173	1.0394	0.98155	1.0794	1.1	1.07641
V11, p.u.	0.96229	1.0866	0.95609	1.02569	1.1	0.99964	1.06079	1.0091	1.0284
V13, p.u.	0.92027	1.1	1.08086	0.98295	0.9512	1.02754	0.98594	1.0398	1.04951
T 6-9, p.u.	0.97118	0.9568	0.94411	1.00036	0.996	1.01241	1.09999	1.1	0.99886
T 6-10, p.u.	1.01248	0.9097	1.03616	0.99955	0.9067	1.09475	1.07552	1.0142	0.95109
T 4-12, p.u.	1.0624	0.9	0.90336	0.96799	0.9	1.06608	1.00395	1.1	0.97847
T 28-27, p.u.	1.01076	1.055	0.94495	1.09931	1.1	1.04232	0.97961	1.0269	0.9515
Q 10, p.u.	9.13189	8.994	8.22457	14.925	2702889	21.5025	27.5035	30	5.49274
Q 24, p.u.	11.7776	6.9347	9.63802	18.0374	16.9813	15.4635	23.2904	5	17.7215
Vse1, p.u.	NA	0.0932	0.06638	NA	0.1	0.04123	NA	0.0565	0.01987
Vse2, p.u.	NA	0.0626	0.06482	NA	0.1	0.03847	NA	0.0572	0.00046
Qse1, deg	NA	91.6182	288.79	NA	0	269.76	NA	32.446	269.09
Qse2, deg	NA	93.1755	166.176	NA	5.22719	48.8095	NA	28.291	127.128
Xse1, p.u.	NA	0.0938	1.37469	NA	0.1	0.05462	NA	0.1	0.04872
Xse1, p.u.	NA	0.0913	0.55047	NA	0.9536	0.07578	NA	0.1	0.07534
Q <sub>GIPFC</sub> , p.u.	NA	NA	0.08371	NA	NA	0.0226	NA	NA	0.07331
fuel cost \$/h	806.431	801.577	800.303	903.752	948.682	950.016	902.648	929.586	937.322
Emission, ton/h	0.26129	0.31781	0.30711	0.22299	0.20496	0.20426	0.21852	0.2071	0.21664
power loss, MW	8.75197	6.3261	11.7233	4.86923	4.01124	5.34889	4.9129	3.4286	3.27188

As in section 2, current injection modeling of GIPFC is mathematically derived and it is being observed that in comparison to power injection modeling of GIPFC, current injection modeling is better technique in terms of mathematical observation. In this section, PIM and CIM model of GIPFC is incorporated in IEEE-30 bus system and from Table 7, they can be easily compared as OPF solution for considered objectives are solved using both the modeling techniques. We can see that generation fuel cost is 798.881\$/h, emission is 0.202061 ton/h and total power loss is 3.18369 MW when CIM of GIPFC is incorporated, which is less than the objectives minimized by PIM of GIPFC and by far the best result obtained for the objectives under the effect of practical constraints. Convergence curve for both the technique is plotted for all three objectives in Figures 8-10. So, it is an evident that with the CIM of GIPFC using proposed AALO algorithm under practical constraints is best approach to solve the optimal power flow problems. It fastens the convergence and initial iteration starts with less objectives value.

Table 7. Comparison of OPF solutions with power injection model and current injection model of GIPFC for IEEE-30 bus system

Variables	Generation fuel cost \$/h		Emission ton/h		Total power loss (MW)	
	PIM OF GIPFC	CIM OF GIPFC	PIM OF GIPFC	CIM OF GIPFC	PIM OF GIPFC	CIM OF GIPFC
PG1, MW	152.1452	126.1154	51.21809	50.47963	71.28296	69.227
PG2, MW	60	44.60762	50	48.96282	25	60
PG5, MW	22.73976	36.04118	29.41447	30.03733	39.5605	29.129
PG8, MW	21.41351	25.84747	21.23589	29.93604	24.03236	29.495
PG11, MW	16.13788	18.54505	28	16.66767	16.76377	22.117
PG13, MW	18.84142	27.88265	35	35.2062	24	24.951
V1, p.u.	0.993978	1.059251	0.982404	1.069144	1.092191	0.976
V2, p.u.	0.967901	1.05023	0.961366	0.962817	0.993921	1.048
V5, p.u.	1.081741	1.051464	0.990584	1.027999	1.043506	0.986
V8, p.u.	1.009599	1.023271	0.981551	1.027177	1.076408	0.957
V11, p.u.	0.956094	1.043279	0.99964	1.076781	1.028397	1.097152
V13, p.u.	1.080862	1.05961	1.027536	1.022123	1.049514	1.041
T6-9, p.u.	0.944109	0.98062	1.01241	0.956076	0.998862	0.921
T6-10, p.u.	1.036162	1.047095	1.09475	0.986248	0.951087	0.95
T4-12, p.u.	0.903357	0.964297	1.066082	0.954205	0.978472	0.986
T28-27, p.u.	0.944948	1.016266	1.042322	0.994694	0.951497	0.964
Q10, p.u.	8.224565	22.33019	21.50248	7.574524	5.492738	20.899
Q24, p.u.	9.638023	25.12324	15.46346	24.43548	17.72147	6.404
Vse1, p.u.	0.066384	0.122422	0.041229	0.83803	0.019865	0.632
Vse2, p.u.	0.064822	0.504409	0.038472	0.148498	0.000464	0.194
θse1, deg	288.7902	246.8979	269.7597	48.10084	269.0895	273.6117
θse2, deg	166.1756	226.4817	48.80947	265.4448	127.1278	338.2553
Xse1, p.u.	1.374693	0.720624	0.054615	0.888889	0.048723	0.592
Xse1, p.u.	0.550469	0.779768	0.075779	0.42209	0.075338	0.335
Xsh, p.u.	NA	1.004626	NA	0.421743	NA	0.964
Vsh, p.u.	NA	0.737168	NA	0.379033	NA	0.574
θsh, p.u.	NA	339.9701	NA	240.79022	NA	272.7
Fuel cost \$/h	800.3032	798.8806	950.0163	968.7877	937.3221	958.1022
Emission, ton/h	0.307109	0.305395	0.204258	0.202061	0.216643	0.275682
Power loss, MW	11.7233	7.217743	5.348887	7.728633	3.271884	3.18369

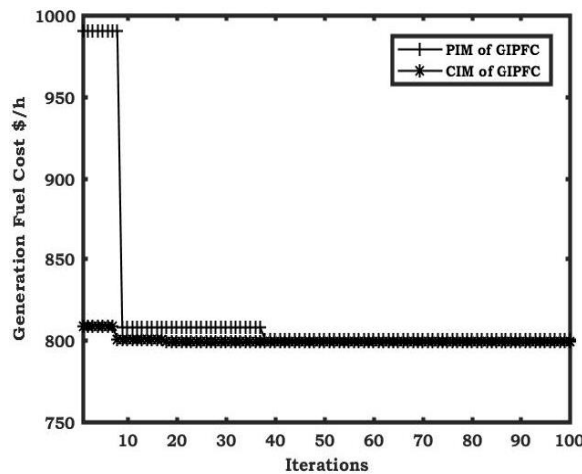


Figure 8. Convergence curve of generation fuel cost with PIM and CIM of GIPFC

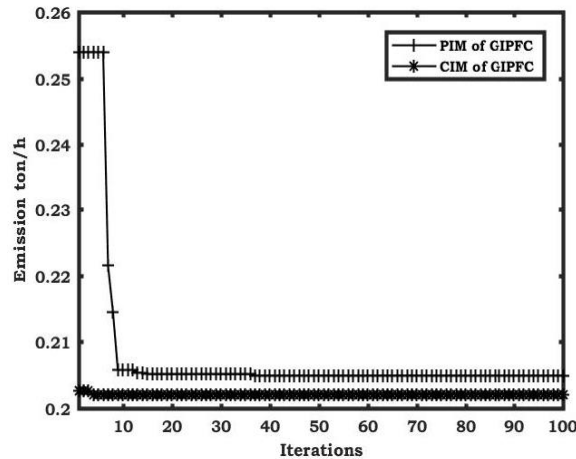


Figure 9. Convergence curve of emission with PIM and CIM of GIPFC

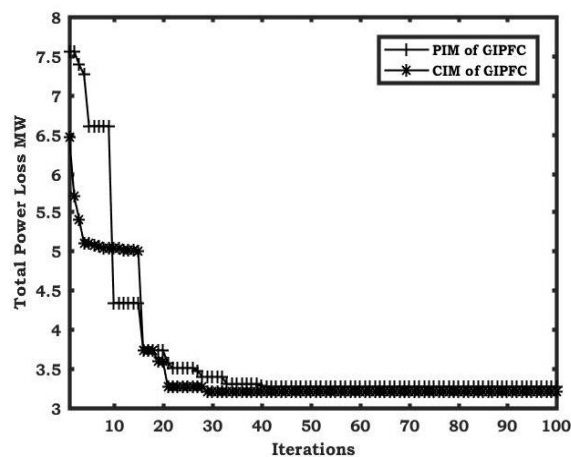


Figure 10. Convergence curve of total power loss with PIM and CIM of GIPFC

## 7. CONCLUSION

In this paper, ameliorated ant lion optimization algorithm had been proposed for minimizing the single as well as multi-objectives problem of OPF including objectives such as generation fuel cost, emission, and total power losses with the incorporation of GIPFC in power system. The proposed algorithm had been tested on Sphere and Rastrigin test functions, which in results proves that the addition of Lévy flight operator in existing ant lion optimization Algorithm revamp the performance and yields better solutions with fast convergence rate. In addition to it, current injection modeling of GIPFC had been derived and implemented in NR load flow method and observed that it is simple and better approach for modeling a series controller as it leads to wider and faster the convergence. For optimal allocation of GIPFC, LSZ formula had been implemented which helps to maintain the voltage stability in power system as it identify the weakest lines which are at a verge to get collapse and those weakest lines had been considered for placing the device. Thus, the proposed algorithm with CIM of GIPFC had been validated on IEEE-30 bus system and hence it can be contemplated as a better alternative approach for solving OPF problems more effectively and efficiently.

## REFERENCES

- [1] Z. Meng, Y. Zhong, G. Mao, and Y. Liang, "PSO-sono: A novel PSO variant for single-objective numerical optimization," *Information Sciences*, vol. 586, pp. 176–191, Mar. 2022, doi: 10.1016/j.ins.2021.11.076.
- [2] D. S. Wais and W. S. Majeed, "The gravitational search algorithm for incorporating TCSC devices into the system for optimum power flow," *International Journal of Electrical and Computer Engineering (IJECE)*, vol. 11, no. 6, pp. 4678–4688, Dec. 2021, doi: 10.11591/ijece.v11i6.pp4678-4688.

- [3] B. Patil and S. B. Karajgi, "Optimized placement of multiple FACTS devices using PSO and CSA algorithms," *International Journal of Electrical and Computer Engineering (IJECE)*, vol. 10, no. 4, pp. 3350–3357, Aug. 2020, doi: 10.11591/ijece.v10i4.pp3350-3357.
- [4] S. Hocine and L. Djamel, "Optimal number and location of UPFC devices to enhance voltage profile and minimizing losses in electrical power systems," *International Journal of Electrical and Computer Engineering (IJECE)*, vol. 9, no. 5, pp. 3981–3992, Oct. 2019, doi: 10.11591/ijece.v9i5.pp3981-3992.
- [5] M. Y. Suliman, "Active and reactive power flow management in parallel transmission lines using static series compensation (SSC) with energy storage," *International Journal of Electrical and Computer Engineering (IJECE)*, vol. 9, no. 6, pp. 4598–4609, Dec. 2019, doi: 10.11591/ijece.v9i6.pp4598-4609.
- [6] H. V. G. Rao, N. Prabhu, and R. C. Mala, "Emulated reactance and resistance by a SSSC incorporating energy storage device," *International Journal of Electrical and Computer Engineering (IJECE)*, vol. 9, no. 2, pp. 840–850, Apr. 2019, doi: 10.11591/ijece.v9i2.pp840-850.
- [7] M. B. Reddy, Y. P. Obulesh, S. Sivanagaraju, and C. V Suresh, "Mathematical modelling and analysis of generalised interline power flow controller: an effect of converter location," *Journal of Experimental & Theoretical Artificial Intelligence*, vol. 28, no. 4, pp. 655–671, Jul. 2016, doi: 10.1080/0952813X.2015.1042529.
- [8] M. Balasubbareddy, "A solution to the multi-objective optimization problem with FACTS devices using NSHCSA including practical constraints," in *2017 IEEE International Conference on Power, Control, Signals and Instrumentation Engineering (ICPCSI)*, Sep. 2017, pp. 2615–2624, doi: 10.1109/ICPCSI.2017.8392190.
- [9] K. Kavitha and R. Neela, "Optimal allocation of multi-type FACTS devices and its effect in enhancing system security using BBO, WIPSO and PSO," *Journal of Electrical Systems and Information Technology*, vol. 5, no. 3, pp. 777–793, Dec. 2018, doi: 10.1016/j.jesit.2017.01.008.
- [10] M. K. Jalboub, H. S. Rajamani, D. T. W. Liang, R. A. Abd-Alhameed, and A. M. Ibbal, "Investigation of voltage stability indices to identify weakest bus (TBC)," in *Mobile Multimedia Communications*, Springer Berlin Heidelberg, 2012, pp. 682–687.
- [11] K. Xie and Y. H. Song, "Dynamic optimal power flow by interior point methods," *IEE Proceedings-Generation, Transmission and Distribution*, vol. 148, no. 1, 2001, doi: 10.1049/ip-gtd:20010026.
- [12] J. Lavei, A. Rantzer, and S. Low, "Power flow optimization using positive quadratic programming," *IFAC Proceedings Volumes*, vol. 44, no. 1, pp. 10481–10486, Jan. 2011, doi: 10.3182/20110828-6-IT-1002.02588.
- [13] J. A. Momoh, R. Adapa, and M. E. El-Hawary, "A review of selected optimal power flow literature to 1993. I. Nonlinear and quadratic programming approaches," *IEEE Transactions on Power Systems*, vol. 14, no. 1, pp. 96–104, 1999, doi: 10.1109/59.744492.
- [14] J. A. Momoh, M. E. El-Hawary, and R. Adapa, "A review of selected optimal power flow literature to 1993. II. Newton, linear programming and interior point methods," *IEEE Transactions on Power Systems*, vol. 14, no. 1, pp. 105–111, 1999, doi: 10.1109/59.744495.
- [15] O. Alsac and B. Stott, "Optimal load flow with steady-state security," *IEEE Transactions on Power Apparatus and Systems*, vol. PAS-93, no. 3, pp. 745–751, May 1974, doi: 10.1109/TPAS.1974.293972.
- [16] D. Sun, B. Ashley, B. Brewer, A. Hughes, and W. Tinney, "Optimal power flow by newton approach," *IEEE Transactions on Power Apparatus and Systems*, vol. PAS-103, no. 10, pp. 2864–2880, Oct. 1984, doi: 10.1109/TPAS.1984.318284.
- [17] S. Mirjalili, S. M. Mirjalili, and A. Lewis, "Grey wolf optimizer," *Advances in Engineering Software*, vol. 69, pp. 46–61, Mar. 2014, doi: 10.1016/j.advengsoft.2013.12.007.
- [18] S. Saremi, S. Z. Mirjalili, and S. M. Mirjalili, "Evolutionary population dynamics and grey wolf optimizer," *Neural Computing and Applications*, vol. 26, no. 5, pp. 1257–1263, Jul. 2015, doi: 10.1007/s00521-014-1806-7.
- [19] M. Kohli and S. Arora, "Chaotic grey wolf optimization algorithm for constrained optimization problems," *Journal of Computational Design and Engineering*, vol. 5, no. 4, pp. 458–472, Oct. 2018, doi: 10.1016/j.jcde.2017.02.005.
- [20] T. Jayabarathi, T. Raghunathan, B. R. Adarsh, and P. N. Suganthan, "Economic dispatch using hybrid grey wolf optimizer," *Energy*, vol. 111, pp. 630–641, Sep. 2016, doi: 10.1016/j.energy.2016.05.105.
- [21] A. A. Heidari and P. Pahlavani, "An efficient modified grey wolf optimizer with Lévy flight for optimization tasks," *Applied Soft Computing*, vol. 60, pp. 115–134, Nov. 2017, doi: 10.1016/j.asoc.2017.06.044.
- [22] D. Karaboga, "Artificial bee colony algorithm," *Scholarpedia*, vol. 5, no. 3, 2010, doi: 10.4249/scholarpedia.6915.
- [23] P.-W. Tsai, J.-S. Pan, B.-Y. Liao, and S.-C. Chu, "Enhanced artificial bee colony optimization," *International Journal of Innovative Computing, Information and Control*, vol. 5, no. 12, pp. 5081–5092, 2009.
- [24] W. Gao and S. Liu, "Improved artificial bee colony algorithm for global optimization," *Information Processing Letters*, vol. 111, no. 17, pp. 871–882, Sep. 2011, doi: 10.1016/j.ipl.2011.06.002.
- [25] G. Zhu and S. Kwong, "Gbest-guided artificial bee colony algorithm for numerical function optimization," *Applied Mathematics and Computation*, vol. 217, no. 7, pp. 3166–3173, Dec. 2010, doi: 10.1016/j.amc.2010.08.049.
- [26] A. H. Gandomi, X.-S. Yang, and A. H. Alavi, "Cuckoo search algorithm: a metaheuristic approach to solve structural optimization problems," *Engineering with Computers*, vol. 29, no. 1, pp. 17–35, Jan. 2013, doi: 10.1007/s00366-011-0241-y.
- [27] M. Tuba, M. Subotic, and N. Stanarevic, "Performance of a modified cuckoo search algorithm for unconstrained optimization problems," *WSEAS Transactions on Systems*, vol. 11, no. 2, pp. 62–74, May 2012, doi: 10.2174/1573405614666180905111128.
- [28] C. A. Roa-Sepulveda and B. J. Pavez-Lazo, "A solution to the optimal power flow using simulated annealing," *International Journal of Electrical Power and Energy Systems*, vol. 25, no. 1, pp. 47–57, Jan. 2003, doi: 10.1016/S0142-0615(02)00020-0.
- [29] T. Sousa, J. Soares, Z. A. Vale, H. Morais, and P. Faria, "Simulated Annealing metaheuristic to solve the optimal power flow," in *2011 IEEE Power and Energy Society General Meeting*, Jul. 2011, pp. 1–8, doi: 10.1109/PES.2011.6039543.
- [30] S. Mirjalili, "The ant lion optimizer," *Advances in Engineering Software*, vol. 83, pp. 80–98, May 2015, doi: 10.1016/j.advengsoft.2015.01.010.
- [31] M. S. Kumari and S. Maheswarapu, "Enhanced genetic algorithm based computation technique for multi-objective optimal power flow solution," *International Journal of Electrical Power and Energy Systems*, vol. 32, no. 6, pp. 736–742, Jul. 2010, doi: 10.1016/j.ijepes.2010.01.010.
- [32] S. Khunkitti, A. Siritariwat, and S. Premrudeepreechacharn, "Multi-objective optimal power flow problems based on slime mould algorithm," *Sustainability*, vol. 13, no. 13, Jul. 2021, doi: 10.3390/su13137448.
- [33] S. Khunkitti, N. R. Watson, R. Chatthaworn, S. Premrudeepreechacharn, and A. Siritariwat, "An improved DA-PSO optimization approach for unit commitment problem," *Energies*, vol. 12, no. 12, Jun. 2019, doi: 10.3390/en12122335.
- [34] S. Khunkitti et al., "A comparison of the effectiveness of voltage stability indices in an optimal power flow," *IEEE Transactions on Electrical and Electronic Engineering*, Dec. 2018, doi: 10.1002/tee.22836.
- [35] S. Khunkitti, A. Siritariwat, S. Premrudeepreechacharn, R. Chatthaworn, and N. Watson, "A hybrid DA-PSO optimization algorithm for multiobjective optimal power flow problems," *Energies*, vol. 11, no. 9, Aug. 2018, doi: 10.3390/en11092270.

- [36] S. Mouassa, T. Bouktir, and A. Salhi, "Ant lion optimizer for solving optimal reactive power dispatch problem in power systems," *Engineering Science and Technology, an International Journal*, vol. 20, no. 3, pp. 885–895, Jun. 2017, doi: 10.1016/j.jestch.2017.03.006.
- [37] M. Jain, V. Singh, and A. Rani, "A novel nature-inspired algorithm for optimization: Squirrel search algorithm," *Swarm and Evolutionary Computation*, vol. 44, pp. 148–175, Feb. 2019, doi: 10.1016/j.swevo.2018.02.013.
- [38] K. Lee, Y. Park, and J. Ortiz, "A united approach to optimal real and reactive power dispatch," *IEEE Transactions on Power Apparatus and Systems*, vol. PAS-104, no. 5, pp. 1147–1153, May 1985, doi: 10.1109/TPAS.1985.323466.
- [39] M. Balasubbareddy, "Multi-objective optimization in the presence of ramp-rate limits using non-dominated sorting hybrid fruit fly algorithm," *Ain Shams Engineering Journal*, vol. 7, no. 2, pp. 895–905, Jun. 2016, doi: 10.1016/j.asej.2016.01.005.
- [40] M. Balasubbareddy, S. Sivanagaraju, and C. V. Suresh, "Multi-objective optimization in the presence of practical constraints using non-dominated sorting hybrid cuckoo search algorithm," *Engineering Science and Technology, an International Journal*, vol. 18, no. 4, pp. 603–615, Dec. 2015, doi: 10.1016/j.jestch.2015.04.005.
- [41] B. Jediti, A. H. Einaddin, and R. Kazemzadeh, "Optimal power flow problem considering the cost, loss, and emission by multi-objective electromagnetism-like algorithm," Jan. 2016, doi: 10.1109/ctpp.2016.7482931.
- [42] A.-F. Attia, R. A. El Sehiemy, and H. M. Hasanien, "Optimal power flow solution in power systems using a novel Sine-Cosine algorithm," *International Journal of Electrical Power and Energy Systems*, vol. 99, pp. 331–343, Jul. 2018, doi: 10.1016/j.ijepes.2018.01.024.
- [43] N. Leeprechanon and P. Phonrattanasak, "Bees two-hive algorithm for optimal power flow," *Applied Mechanics and Materials*, vol. 313–314, pp. 870–875, Mar. 2013, doi: 10.4028/www.scientific.net/AMM.313-314.870.
- [44] T. Niknam, M. rasoul Narimani, M. Jabbari, and A. R. Malekpour, "A modified shuffle frog leaping algorithm for multi-objective optimal power flow," *Energy*, vol. 36, no. 11, pp. 6420–6432, Nov. 2011, doi: 10.1016/j.energy.2011.09.027.
- [45] R. Arul, G. Ravi, and S. Velusami, "Solving optimal power flow problems using chaotic self-adaptive differential harmony search algorithm," *Electric Power Components and Systems*, vol. 41, no. 8, pp. 782–805, 2013, doi: 10.1080/15325008.2013.769033.
- [46] V. Yadav and S. P. Ghoshal, "Optimal power flow for IEEE 30 and 118-bus systems using Monarch Butterfly optimization," in *2018 Technologies for Smart-City Energy Security and Power (ICSESP)*, 2018, pp. 1–6, doi: 10.1109/ICSESP.2018.8376670.
- [47] G. Chen, S. Qiu, Z. Zhang, Z. Sun, and H. Liao, "Optimal power flow using gbest-guided cuckoo search algorithm with feedback control strategy and constraint domination rule," *Mathematical Problems in Engineering*, vol. 2017, pp. 1–14, 2017, doi: 10.1155/2017/9067520.
- [48] A. A. Abou El Ela, M. A. Abido, and S. R. Spea, "Optimal power flow using differential evolution algorithm," *Electric Power Systems Research*, vol. 80, no. 7, pp. 878–885, Jul. 2010, doi: 10.1016/j.epr.2009.12.018.
- [49] M. A. Abido, "Optimal power flow using tabu search algorithm," *Electric Power Components and Systems*, vol. 30, no. 5, pp. 469–483, May 2002, doi: 10.1080/15325000252888425.
- [50] U. Kılıç, "Backtracking search algorithm-based optimal power flow with valve point effect and prohibited zones," *Electrical Engineering*, vol. 97, no. 2, pp. 101–110, Jun. 2015, doi: 10.1007/s00202-014-0315-0.
- [51] L. Slimani and T. Bouktir, "Economic power dispatch of power systems with pollution control using artificial bee colony optimization," *Turkish Journal of Electrical Engineering and Computer Sciences*, vol. 21, pp. 1515–1527, 2013, doi: 10.3906/elk-1106-10.
- [52] S. Duman, U. Güvenç, Y. Sönmez, and N. Yörükere, "Optimal power flow using gravitational search algorithm," *Energy Conversion and Management*, vol. 59, pp. 86–95, Jul. 2012, doi: 10.1016/j.enconman.2012.02.024.
- [53] A. Bhattacharya and P. K. Chattopadhyay, "Application of biogeography-based optimisation to solve different optimal power flow problems," *IET Generation, Transmission and Distribution*, vol. 5, no. 1, 2011, doi: 10.1049/iet-gtd.2010.0237.

## BIOGRAPHIES OF AUTHORS



**Mallala Balasubbareddy**     research focuses on Optimization Techniques, IoT, smart grid, design of Photovoltaic systems and electrical distribution analysis. He uses MATLAB programming and optimization techniques including Hardware experience design of PV systems with SCADA control. Three projects were executed with off grid and on grid systems with support of Solar Energy Corporation of India (SECI). In collaboration with a Chennai based company Industrial Controls and Drives (India) Pvt. Ltd. (ICD), his team has developed an energy management system for integrating grid and solar power generation capacity of 400 kWp at SV Colleges, Tirupati (Previous working College). He published significant number of referred journals in the area of multi-objective optimization techniques and design of solar energy systems. He can be contacted at email: [balasubbareddy79@gmail.com](mailto:balasubbareddy79@gmail.com).



**Divyanshi Dwivedi**     received the Bachelor of Engineering degree in Electrical and Electronics Engineering, Master's degree from CBIT, Hyderabad. Currently, she is scholar at Indian Institute of Technology, Hyderabad. She published several publications in international journals and conferences. Her area of interests is in power system, renewable energy resources, complex network theory, machine learning algorithm implementation in power system operation and control, optimization techniques and FACTS controllers. She can be contacted at email: [divyanshidw@gmail.com](mailto:divyanshidw@gmail.com).



**Garikamukkala Venkata Krishna Murthy**    obtained his B.E degree in Electrical and Electronics Engineering from UCE, Andhra University, Visakhapatnam, India in 1999. He obtained his M.Tech degree in Electrical Power Engineering from UCE, J.N.T. University, Hyderabad, India and did his Ph.D. from J.N.T. University, Kakinada, India. He is presently working as Professor and Head in the Department of Electrical and Electronics Engineering in PACE Institute of Technology and Sciences, Ongole, Andhra Pradesh, India. His areas of interest are power systems, electrical distribution systems and electrical machines. He can be contacted at email: murthy260@gmail.com.



**Kotte Sowjan Kumar**    obtained his B.Tech. degree in Electrical and Electronics Engineering from AGCET Tadepalligudem, JNTU Hyderabad, India in 2005. He obtained his M.Tech degree in Electrical Engineering from IIT, IIT Kharagpur in 2010, India. He is presently working as associate Professor in the Department of Electrical and Electronics engineering, PACE Institute of Technology and Sciences, Ongole, Andhra Pradesh, India. His areas of interest are power systems, renewable energy sources and smart grids. He can be contacted at email: sowji212@gmail.com.